

Submitted to *The Astrophysical Journal*, 22 March 1998

Neutron Star Mass Measurements. I. Radio Pulsars

S. E. Thorsett¹

Joseph Henry Laboratories and Department of Physics, Princeton University,
Princeton, NJ 08544; steve@pulsar.princeton.edu

and

Deepto Chakrabarty²

Center for Space Research, Massachusetts Institute of Technology, Cambridge, MA 02139;
deepto@space.mit.edu

ABSTRACT

There are now about fifty known radio pulsars in binary systems, including at least five in double neutron star binaries. In some cases, the stellar masses can be directly determined from measurements of relativistic orbital effects. In others, only an indirect or statistical estimate of the masses is possible. We review the general problem of mass measurement in radio pulsar binaries, and critically discuss all current estimates of the masses of radio pulsars and their companions. We find that significant constraints exist on the masses of twenty-one radio pulsars, and on five neutron star companions of radio pulsars. All the measurements are consistent with a remarkably narrow underlying gaussian mass distribution, $m = 1.35 \pm 0.04 M_{\odot}$. There is no evidence that extensive mass accretion ($\Delta m \gtrsim 0.1 M_{\odot}$) has occurred in these systems. We also show that the observed inclinations of millisecond pulsar binaries are consistent with a random distribution, and thus find no evidence for either alignment or counteralignment of millisecond pulsar magnetic fields.

Subject headings: stars: neutron — stars: masses — pulsars: general

¹Alfred P. Sloan Research Fellow

²NASA Compton GRO Postdoctoral Fellow

1. Introduction

Neutron stars have been the subject of considerable theoretical investigation since long before they were discovered as astronomical sources of radio and X-ray emission (Baade and Zwicky 1934, Oppenheimer and Volkoff 1939, Wheeler 1966). Their properties are determined by the interplay of all four known fundamental forces—electromagnetism, gravitation, and the strong and weak nuclear forces—but neutron stars remain sufficiently simple in their internal structure that realistic stellar modeling can be done. Measurements of their masses and radii (as well as detailed study of their cooling histories and rotational instabilities) provide a unique window on the behavior of matter at densities well above that found in atomic nuclei ($\rho_{\text{nuc}} \approx 2.8 \times 10^{14} \text{g cm}^{-3}$). Observations of neutron stars also provide our only current probe of general relativity (GR) in the “strong-field” regime, where gravitational self-energy contributes significantly to the stellar mass.

The most precisely measured physical parameter of any pulsar is its spin frequency. The frequencies of the fastest observed pulsars (PSR B1937+21 at 641.9 Hz and B1957+20 at 622.1 Hz) have already been used to set constraints on the nuclear equation of state at high densities (e.g., Friedman *et al.* 1988) under the assumption that these pulsars are near their maximum (breakup) spin frequency. However, the fastest observed spin frequencies may be limited by complex accretion physics rather than fundamental nuclear and gravitational physics. A quantity more directly useful for comparison with physical theories is the neutron star mass.

The basis of most neutron star mass estimates is the analysis of binary motion. Soon after the discovery of the first binary radio pulsar (Hulse and Taylor 1975), it became clear that the measurement of relativistic orbital effects allowed extremely precise mass estimates. Indeed, the measurement uncertainties in several cases now exceed in precision our knowledge of Newton’s constant G , requiring masses to be quoted in solar units GM_{\odot} rather than kilograms if full accuracy is to be retained.

After several recent pulsar surveys, there are now about fifty known binary radio pulsar systems, of which five or six are thought to contain two neutron stars. It is thus possible for the first time to consider compiling a statistically significant sample of neutron star masses. It is our purpose here to provide a general, critical review of all current estimates of stellar masses in radio pulsar binaries. The resulting catalog, with a careful, uniform approach to measurement and systematic uncertainties, should be of value both to those who wish to apply mass measurements to studies of nuclear physics, GR, and stellar evolution, and as a guide to the critical observations for observational pulsar astronomers. We begin with a discussion of known methods for pulsar mass determination (§2), including a new statistical technique for estimating the masses of millisecond pulsars in non-relativistic systems. In §3

we review all known mass estimates, including new data and analysis where possible. Statistical analysis of the available pulsar mass measurements is presented in §4. We summarize in §5.

A second paper will consider mass estimates for neutron stars in X-ray binary systems (Chakrabarty and Thorsett 1998, Paper II). A detailed discussion of the implications of the combined results of this work and Paper II for studies of supernovae and neutron star formation, mass transfer in binary evolution, the nuclear equation of state, and GR will occur elsewhere (Paper III).

2. Methods of mass estimation

It is a familiar circumstance that estimates of astronomical masses are available only for bodies in gravitationally bound binary systems or clusters. Compact stars introduce the additional possibility of directly measuring the surface gravitational potential, and hence M/R , through the study of redshifted spectral features. Although this technique has been used with considerable success in the case of white dwarfs, and attempts have been made to fit redshifted X-ray spectra from neutron stars (Paper II), no lines have been identified in radio pulsar spectra and other gravitational effects on the observed emission from pulsars are sufficiently complex and theory dependent that no useful limits on the neutron star properties have yet been possible. In the following, we thus limit ourselves only to the determination of stellar masses in binary systems.

2.1. Pulsar timing

In any binary pulsar system, five Keplerian parameters can be very precisely measured by pulse timing techniques (Manchester and Taylor 1977): the binary period P_b , the projection of the pulsar’s semimajor axis on the line of sight $x \equiv a_1 \sin i/c$ (where the binary inclination i is the angle between the line of sight and the orbital angular momentum vector, defined to lie in the first quadrant), the eccentricity e , and the time and longitude of periastron, T_0 and ω_0 . It is frequently more convenient to use the orbital angular frequency in place of the orbital period: $n \equiv 2\pi/P_b$. These observational parameters are related to the pulsar and companion masses, m_1 and m_2 , through the mass function

$$f = \frac{(m_2 \sin i)^3}{M^2} = n^2 x^3 \left(\frac{1}{T_\odot} \right) M_\odot, \quad (1)$$

where $M \equiv m_1 + m_2$, the masses are measured in solar units, and we introduce the constant $T_\odot \equiv GM_\odot/c^3 = 4.925\,490\,947 \times 10^{-6}$ s.

Relativistic corrections to the binary equations of motion are most often parameterized in terms of one or more post-Keplerian (PK) parameters (Damour and Deruelle 1986, Taylor and Weisberg 1989, Damour and Taylor 1992). In GR, the most significant PK parameters have familiar interpretations as the advance of periastron of the orbit $\dot{\omega}$, the combined effect of variations in the transverse Doppler shift and gravitational redshift around an elliptical orbit γ , the orbital decay due to emission of quadrupole gravitational radiation \dot{P}_b , and the “range” and “shape” parameters r and s that characterize the Shapiro time delay of the pulsar signal as it propagates through the gravitational field of its companion. In terms of measured quantities and the pulsar and companion masses (in solar units), these PK parameters are given by (Taylor 1992):

$$\dot{\omega} = 3n^{\frac{5}{3}} (T_\odot M)^{\frac{2}{3}} (1 - e^2)^{-1}, \quad (2)$$

$$\gamma = en^{-\frac{1}{3}} T_\odot^{\frac{2}{3}} M^{-\frac{4}{3}} m_2 (m_1 + 2m_2), \quad (3)$$

$$\dot{P}_b = -\frac{192\pi}{5} n^{\frac{5}{3}} \left(1 + \frac{73}{24}e^2 + \frac{37}{96}e^4\right) (1 - e^2)^{-\frac{7}{2}} T_\odot^{\frac{5}{3}} m_1 m_2 M^{-\frac{1}{2}}, \quad (4)$$

$$r = T_\odot m_2, \quad (5)$$

$$s = xn^{\frac{2}{3}} T_\odot^{-\frac{1}{3}} M^{\frac{2}{3}} m_2^{-1}. \quad (6)$$

Note, by combining equations (1) and (6), that $s = \sin i$ for GR.)

The measurement of the mass function f (equation 1) together with any two PK parameters (equations 2–6) is sufficient in the context of GR to uniquely determine the component masses m_1 and m_2 . With additional assumptions, such as a uniform prior likelihood for orbital orientations with respect to the observer (§2.3.4), strong statements about the posterior distribution of the masses is often possible if even a single PK parameter is measured.

As an alternative to the PK formalism, which is designed for testing gravitation theory, it is sometimes advantageous to fit the timing data to a model that *assumes* the correctness of GR. For example, the DDGR model of Damour, Deruelle, and Taylor (Taylor 1987, Taylor and Weisberg 1989) describes the pulsar phase as a function of the five Keplerian parameters, the companion mass m_2 , and the total mass M . A least-squares fit of the timing data to the DDGR model thus gives direct estimates of the uncertainties in m_2 and M , as well as the covariances between the mass estimates and estimates of other parameters.

It is of interest to note that mass measurements from pulsar timing observations depend on the unknown relative motion of the solar system and the binary barycenters. Damour and Deruelle (1986) have shown that neglecting this velocity is equivalent to changing units

of mass and time. In particular, the rest frame mass m and the barycenter frame mass m^{ssb} are related by $m = Dm^{\text{ssb}}$, with Doppler factor

$$D \equiv \frac{1 - \hat{\mathbf{n}} \cdot \mathbf{v}_b/c}{\sqrt{1 - v_b^2/c^2}}, \quad (7)$$

where $\hat{\mathbf{n}}$ is the line of sight unit vector and \mathbf{v}_b is the barycentric velocity of the pulsar. Although the transverse velocity of the binary system can be estimated from proper motion measurements, the radial component $\hat{\mathbf{n}} \cdot \mathbf{v}_b$ is unknown. For a typical velocity of 100 km s^{-1} , the systematic mass error is about $\sim 0.03\%$; small, but in some cases much larger than other uncertainties.

2.2. Masses of companion stars

While timing measurements of relativistic corrections to the Keplerian orbital equations provide the most accurate and theory-independent estimates of neutron star masses, they are possible only for close, eccentric binary orbits or when the orbit is observed nearly edge-on. In the great majority of observed binaries, the mass function provides the only timing information about the component masses, and the pulsar mass can only be determined if additional constraints are found on the companion mass and binary inclination through other techniques. This section describes several ways to use observations or theoretical considerations to limit m_2 ; alternate limits on $\sin i$ are the topic of §2.3.

2.2.1. Optical observations of white dwarf companions

In recent years, over a dozen companion stars in radio pulsar binaries have been optically detected (e.g., van Kerkwijk 1996, Lundgren, Camilo, and Foster 1996). In most cases, the companions are white dwarfs; the two main sequence exceptions are discussed in the next section. Many of the white dwarf companions are extremely faint ($m_V \sim 26$), allowing detection only with the *Hubble Space Telescope* and the largest ground-based telescopes.

There are a number of ways to determine white dwarf masses (e.g., Reid 1996 and references therein). Given a theoretical relation between the white dwarf mass and radius, the measurement of any combination of the mass and radius is sufficient to determine the mass. For example, the radius can be estimated directly from estimates of the optical flux, effective temperature, and distance. Alternately, the surface gravity, $\log g$, can be found by fitting a model atmosphere to the observed spectrum (Bergeron, Wesemael, and Fontaine 1991), and combining the result with a temperature or luminosity estimate. In practice, difficulties

arise from several sources. First, the white dwarf companions of millisecond pulsars, with typical masses $m_2 < 0.5M_\odot$, are usually believed to be helium white dwarfs which were insufficiently massive to burn to carbon; the luminosity and temperature evolution of such stars has received much less study than for more massive white dwarfs (e.g., D’Antona and Mazzitelli 1990), leading to uncertainties in the finite temperature contributions to the mass-radius relationship. Hansen and Phinney (1998a,b) have recently calculated cooling curves for helium core dwarfs, using their own calculations of H and He opacities at temperatures below 6000 K, and applied their results to a number of radio pulsar companions. We discuss their results in more detail in §3.

The measurement of surface gravity in cool stars is also potentially problematic. A higher helium abundance, as may occur through enhanced convective mixing in cool stars, will produce higher pressure and broader lines and hence mimic a higher white dwarf mass (Bergeron, Wesemael, and Fontaine 1991); indeed, there is some evidence that surface gravity measurements overestimate masses below about 12,000 K (Reid 1996).

2.2.2. *Optical observations of main sequence companions*

Two pulsars have been found in binaries with main sequence companions: PSR B1259–63, with a Be companion (Johnston *et al.* 1992), and PSR J0045–7319, with a B star companion (Kaspi *et al.* 1994). Although in both cases the optical companion is quite bright and easily observed, knowledge of the companion mass m_2 and pulsar mass function f is of little use in limiting m_1 when $m_1 \ll m_2$. If the mass function of the companion can also be measured, then the mass ratio can be determined. This has been done in the case of J0045–7319 (§3.3.1).

2.2.3. *The P_b – m_2 relation*

The binary millisecond pulsars are believed to be spun up to high spin frequencies through mass transfer from a companion star. In many cases, these pulsars are observed in wide, low-eccentricity binary systems with white dwarf secondaries. These characteristics indicate that the secondary must have passed through a red giant phase after the formation of the neutron star primary, during which tidal torques circularized the orbit and the giant probably filled its Roche lobe, causing the mass transfer which spun up the pulsar to millisecond periods. At the end of mass transfer, the envelope of the giant is exhausted or ejected, leaving the degenerate core as a white dwarf secondary. There is a close relation

between the core mass and the radius of low mass giants (Refsdal and Weigert 1971, Web-bink, Rappaport, and Savonije 1983, Joss, Rappaport, and Lewis 1987, Rappaport *et al.* 1995, Rappaport and Joss 1997). Combined with the assumption that the giant filled its Roche lobe during the mass transfer, this yields a relation between the binary period at the end of mass transfer and the remnant white dwarf mass (Rappaport *et al.* 1995).

Following Rappaport *et al.* (1995) and references therein, the relation between the effective radius of the Roche lobe R_L and the binary separation a can be written

$$R_L \approx 0.46 a \left(1 + \frac{m_1}{m_g}\right)^{-1/3}, \quad (8)$$

where m_g is the total mass of the giant (core and envelope). Near the end of mass transfer, the envelope mass can be neglected, so that $m_g \approx m_2$ (where m_2 is the final white dwarf mass), and the giant radius $R_g \approx R_L$. Using Kepler’s third law,

$$P_b = 0.374 R_g^{3/2} m_2^{-1/2} \quad \text{days}, \quad (9)$$

where R_g and m_2 are in solar units. We note that equation (9) is independent of the pulsar mass m_1 , and relates the orbital period at the end of mass transfer to the final white dwarf mass and the giant radius R_g . The radius depends, in general, on the composition and history of the giant as well as on m_2 ; the utility of equation (9) derives from the relatively narrow distribution of R_g for a given m_2 .

Rappaport *et al.* (1995) have examined stellar models with a wide range of chemical compositions, varying between Population I and Population II values, as well as a variety of envelope masses and convective mixing lengths. Over a wide range of core masses greater than $0.15M_\odot$, they find the data are well described by the equation

$$R_g = \frac{R_0 m_2^{4.5}}{1 + 4 m_2^4} + 0.5 \quad (10)$$

where $R_0 = 4950R_\odot$ is the best fit to the stellar models. In all models studied by Rappaport *et al.*, equation (10) was correct within a factor of 1.8. Over the limited range $m_2 < 0.25M_\odot$, Rappaport and Joss (1997) found that the alternate expression

$$\log R_g = 0.031 + 1.718 m_2 + 8.04 m_2^2 \quad (11)$$

could be used, with the smaller uncertainty of a factor ~ 1.3 . We regard these to be approximately 95% confidence regions for R_g .

It is important to determine the range of applicability of equations (10) and (11). At orbital periods less than a few days, heating of the surface of the companion by X-rays

produced during accretion may cause significant bloating and modification of the core mass–radius relations (Podsiadlowski 1991, Rappaport *et al.* 1995). Following Rappaport *et al.*, we trust the modeling only for binary orbits longer than three days. Further, the P_b – m_2 relation cannot be applied to systems like PSR J2145–0750 or J1022+10—both 16 ms pulsars that were most likely recycled in common envelopes that occurred when their companions overflowed their Roche surfaces while on the asymptotic giant branch, leaving carbon-oxygen rather than helium white dwarfs (van den Heuvel 1994)—or to pulsars like B0820+02, a slow (0.864 s), high-field (3×10^{11} G) pulsar without evidence of significant recycling. To avoid both classes of pulsar without introducing biases by cutting on apparent companion mass, we apply the P_b – m_2 relation only to pulsars with $P < 10$ ms, for which the assumption of an extended period of mass transfer during a low-mass X-ray binary phase seems secure.

Using equations (9)–(11), the observed orbital period in a millisecond pulsar binary can be used to limit the range of m_2 . When combined with the mass function (equation 1) and the restriction $\sin i < 1$, an upper limit can be placed on the pulsar mass. The resulting limits are discussed below, in §3.2. If a random distribution of orbits is assumed for the set of observed millisecond pulsars, then statistical arguments lead to limits on the masses of millisecond pulsars as a class. These arguments are described in §4.

2.3. Alternative methods of estimating the orbital inclination

If the companion mass can be estimated and bounds can be found on the orbital inclination, then the mass of the pulsar can be found using the Keplerian mass function. In this section, we discuss measurements that may allow direct estimates of $\sin i$.

2.3.1. Polarization measurements

In the standard model of millisecond pulsar formation, the pulsar is spun-up by mass transfer from a companion star. After spin-up, the pulsar spin axis will be aligned with the orbital angular momentum, so a measurement of the angle ζ between the pulsar spin axis and the line of sight also determines the orbital inclination: $i = \zeta$, or $i = \pi - \zeta$ for ζ in the second quadrant. (Although this is also true at an early stage of the formation of double neutron star binaries, an asymmetry in the second supernova explosion may leave the spin and orbit misaligned.)

In the rotating vector model of pulsar emission, the radio signal is elliptically polarized with the major axis of the polarization ellipse aligned with the plane of curvature of the

dipolar magnetic field lines. The position angle of the observed linear polarization ψ can be expressed as a function of the rotational phase ϕ of the pulsar:

$$\tan(\psi(\phi) - \psi_0) = \frac{\sin \alpha \sin \phi}{\sin \zeta \cos \alpha - \cos \zeta \sin \alpha \cos \phi}, \quad (12)$$

where α is the angle between the pulsar spin axis and the magnetic pole. In practice, the difference $\zeta - \alpha$ can often be estimated quite well from equation (12), but accurate estimates of ζ or α are possible only if polarized emission can be detected over a broad range of pulse phase ϕ .

Application of equation (12) to millisecond pulsars, in which the light cylinder bounds the magnetosphere at only a few stellar radii, may be complicated by multipolar field geometries, aberration, and other deviations from the simple rotating vector model. Indeed, attempts to fit equation (12) to millisecond pulsar data have met with few unqualified successes (Thorsett and Stinebring 1990, Navarro *et al.* 1997).

2.3.2. Interstellar Scintillation

Observed pulsar signal strengths vary in both frequency and time because of scintillation in the interstellar medium. A phase-changing screen along the line of sight produces an interference pattern across which the pulsar moves; the characteristic scintillation decorrelation timescale τ_{iss} is inversely proportional to the transverse component of the pulsar velocity. Observations of scintillation rates have been widely used to estimate the proper motions of isolated pulsars (e.g., Cordes 1986). In binary systems, the transverse velocity is modulated by the orbital motion, with a small amplitude of modulation for orbits viewed face-on, and a large amplitude for orbits viewed on edge. Scintillation measurements can thus provide an alternate path to estimating the inclination angle $\sin i$ (Lyne 1984).

The real physical situation is more complex. The measured scintillation velocity \mathbf{v}_{iss} of a pulsar depends not only on its proper motion \mathbf{v}_{pm} and orbital motion $\mathbf{v}_{\text{orb}}(t)$, but also on the Earth's motion $\mathbf{v}_{\oplus}(t)$, the mean motion of the scattering medium \mathbf{v}_{ism} and the ratio of the effective distance to the scattering screen to the pulsar distance, f :

$$\mathbf{v}_{\text{iss}}(t) = (1 - f)(\mathbf{v}_{\text{orb}}(t) + \mathbf{v}_{\text{pm}}) + f\mathbf{v}_{\oplus}(t) - \mathbf{v}_{\text{ism}}. \quad (13)$$

If the proper motion is known, from timing measurements or interferometry, then the annual modulation of \mathbf{v}_{\oplus} and the orbital modulation of \mathbf{v}_{orb} can in principle be used to find not only the orbital inclination $\sin i$ but also f , the pulsar distance d , and the position angle on the sky of the orbital ascending node Ω .

Only a few attempts to determine orbital inclinations from scintillation observations have been published. In no case was \mathbf{v}_{pm} known, nor has the annual modulation due to \mathbf{v}_{\oplus} been measured (although the latter has been observed in the isolated millisecond pulsar B1937+21 by Ryba (1991)). Lyne (1984) found that the inclination of PSR B0655+64 is either 62° or 84° (the discrete ambiguity could be broken through observations at another time of year, using variations in \mathbf{v}_{\oplus}). Jones and Lyne (1988) later expressed reservations about this measurement. In the most convincing success of the scintillation technique, Dewey *et al.* (1988) found a limit on the the inclination of PSR B1855+09: $\sin i \geq 0.94$. Shapiro time delay measurements have since shown that $\sin i \approx 0.9993$ (§3.2.7).

The problem of estimating scintillation parameters from data is considered by Cordes (1986). The dominant error source in estimating scintillation parameters is the finite number N of scintillation features sampled: $\sigma_v/v_{\text{iss}} \approx 0.6/\sqrt{N}$. Scintillation intensity fluctuations are exponentially distributed; for observing bandwidth B and time T , we have roughly $N \approx 10^{-2}BT/(\Delta\nu_{\text{iss}}\tau_{\text{iss}})$. Considering a case relevant to many recently discovered pulsar binaries, a pulsar at a dispersion measure $\text{DM}=20$ will have typical scintillation parameters at 430 MHz $\tau_{\text{iss}} \sim 10$ minutes and $\Delta\nu_{\text{iss}} \sim 100$ kHz (Rickett 1988). With $B = 10$ MHz and $T = 1$ hr, $\sigma_v/v_{\text{iss}} \sim 25\%$, so a study of orbital dependence of scintillation parameters requires a substantial amount of observing time. Furthermore, to use a bandwidth of 10 MHz requires a spectrometer with $\gtrsim 100$ frequency channels. Such observations will be more easily done with the new generation of flexible, all-digital pulsar data recorders (Shrauner *et al.* 1996, Jenet *et al.* 1997). It is possible that long term variability in f or \mathbf{v}_{iss} will limit the use of the annual variation in \mathbf{v}_{\oplus} to estimate f .

2.3.3. Secular variation of $x = a_1 \sin i$

Proper motion of the binary system across the sky leads to a secular change in the projected semimajor axis x . If Ω is the position angle of the ascending node and μ_α and μ_δ are the components of the proper motion $\boldsymbol{\mu}$ in right ascension and declination, then

$$\frac{\dot{x}}{x} = \cot i (-\mu_\alpha \sin \Omega + \mu_\delta \cos \Omega). \quad (14)$$

The angle Ω is generally unknown (though it is accessible to scintillation measurements, §2.3.2), but eqn. 14 can be rewritten as the limit

$$\tan i < \left| \frac{x}{\dot{x}} \boldsymbol{\mu} \right|. \quad (15)$$

A similar expression can be found relating proper motion to a purely geometric advance of periastron $\dot{\omega}$ —in principle, measurement of both \dot{x} and $\dot{\omega}$ would determine i —but the effect

is too small to have yet been seen in any pulsar binary.

2.3.4. *Random distribution of orbital inclinations*

When no other information is available on the orbital inclination, it is sometimes useful in statistical calculations to assume that binary orbits are randomly oriented with respect to the line of sight. The differential distribution of inclinations is then proportional to $\sin i$ (i.e., the most likely orbital viewing angle is edge-on). Values of $\cos i$ should then be uniformly distributed between 0 and 1.

In binary systems where the directions of the pulsar spin axis and the orbital angular momentum vector are expected to be correlated, such as millisecond pulsar systems in which significant mass transfer has occurred since the last supernova, non-random orientations of the pulsar magnetic field axis with respect to the spin axis may lead to a pulsar discovery bias that skews the observed orbital orientation distribution. Some models of pulsar evolution predict magnetic field alignment, counteralignment, or both (e.g., Ruderman 1991).

Backer (1998) has claimed, based on the distribution of observed mass functions in 21 pulsar–white-dwarf binaries, that millisecond pulsars have a non-random distribution of observed binary inclinations. He suggests that an apparent preference for high inclination orbits may arise because the pulsars’ magnetic fields are preferentially oriented perpendicular to the spin axis. However, his analysis makes several assumptions and approximations that prove unwarranted. In particular, he compares the observed distribution of minimum companion masses $m_{2,\min}$ with the predicted distribution given the observed mass functions, random inclinations and a single fixed value for the true companion masses m_2 (i.e., a delta function distribution in m_2), finding poor agreement. However, the predicted distribution for $m_{2,\min}$ actually depends quite sensitively upon the assumed distribution for m_2 ; the delta function distribution is an unreasonable assumption. Indeed, the P_b – m_2 relation suggests that the observed m_2 values should vary by a factor of three. Knowing the precise limits and distribution of these masses is crucial for analyzing the distribution of $m_{2,\min}$.

We repeated Backer’s analysis, with different assumptions about the distribution of m_2 values. If we assume the true values m_2 fall uniformly in the range 0.15–0.35 M_\odot , then the predicted and observed distributions for $m_{2,\min}$ agree at an 81% confidence level according to a Kolmogorov-Smirnov (KS) test (e.g., Eadie *et al.* 1971). However, assuming a 0.1–0.4 M_\odot range reduces the agreement to the 33% confidence level. The discrepancy is primarily due to a deficit of observed systems with small values of $m_{2,\min}$, as noted by Backer. Unfortunately, our knowledge of the true underlying distribution of m_2 in these binaries is sufficiently

uncertain that no conclusion regarding the distribution of inclinations is possible from this line of analysis. However, we argue below (§4) that for systems with orbital periods longer than three days, where the P_b – m_2 relation can be applied to estimate the m_2 distribution, the observed mass functions are consistent with a random distribution of inclinations.

3. Radio pulsar masses

The parameters of 47 radio pulsar binary systems are listed in Table 1. At least five of these pulsars have neutron star companions, so a total of 52 neutron stars are known in radio pulsar binaries. Useful mass constraints can be placed on half of these stars.

3.1. Double neutron star binaries

3.1.1. PSR J1518+4904

PSR J1518+4904 is in a moderately relativistic binary system; one PK parameter has been measured, the relativistic advance of periastron $\dot{\omega} = 0.0111(2)^\circ\text{yr}^{-1}$, yielding a total system mass of $2.62(7)M_\odot$ (Nice, Sayer, and Taylor 1996). Given the mass function $f = 0.115988M_\odot$, the lower limit on the companion mass (using $\sin i < 1$) is $m_2 > (fM^2)^{1/3} = 0.93M_\odot$, and the lower limit on the inclination (given $m_1 > 0$) is $\sin i > (f/M)^{1/3} = 0.35$ (or $i > 20^\circ$). Using a uniform prior distribution in $\sin i$ over the interval $0.35 < \sin i < 1$, we find the central 68% confidence intervals $m_1 = 1.56^{+0.13}_{-0.44}$ and $m_2 = 1.05^{+0.45}_{-0.11}$ and central 95% confidence intervals $m_1 = 1.56^{+0.20}_{-1.20}$ and $m_2 = 1.05^{+1.21}_{-0.14}$.

The identification of the companion as a neutron star is compelling, although it is not possible to completely rule out a low-mass black hole. Optical observations (van Kerkwijk, quoted in Sayer 1996) show no source at the pulsar position to $m_B \sim 24.5$, excluding a main sequence companion, and a white dwarf in an eccentric orbit is not expected on evolutionary grounds.

3.1.2. PSR B1534+12

PSR B1534+12 is in a highly relativistic binary system, presumably with a second neutron star companion. All five of the PK parameters defined by equations (2)–(6) have been measured, three with better than 1% precision (Stairs *et al.* 1998). Using the DDGR timing model, the total system mass is found to be $M = 2.67838(8)M_\odot$, while the individual

component masses m_1 and m_2 are both $1.339(3)M_\odot$. (The quoted errors are 68% confidence regions; the 95% confidence regions are about twice as large.) It is remarkable that the pulsar and companion masses agree to better than 0.4%; the assumption that the companion is a second neutron star seems secure. The uncertainty on the individual masses is expected to decrease significantly in the next year, when observations are again possible with the Arecibo telescope.

3.1.3. PSR B1913+16

PSR B1913+16 was the first binary pulsar discovered and, with observations stretching over two decades, it remains one of the best studied. PSR B1913 is a highly relativistic system: the PK parameters $\dot{\omega}$, γ , and \dot{P}_b have all been measured precisely. A fit to the DDGR timing model yields the total system mass $M = 2.82843(2)$ and component masses $m_1 = 1.4411(7)$ and $m_2 = 1.3874(7)M_\odot$ (Taylor 1992). (The quoted errors are 68% confidence regions; the 95% confidence regions are about twice as large.) The uncertainties are approaching the level where they will be dominated by kinematic effects (equation 7).

3.1.4. PSR B2127+11C

PSR B2127+11C is a relativistic binary in the globular cluster M15. Precise measurements have been made of the PK parameters $\dot{\omega}$ and γ , resulting in mass estimates for the pulsar and companion of $1.349(40)$ and $1.363(40)M_\odot$, respectively, and a total system mass $M = 2.7121(6)M_\odot$ (Deich and Kulkarni 1996). (The quoted errors are 68% confidence regions; the 95% confidence regions are approximately twice as large.)

3.1.5. PSR B2303+46

PSR B2303+46 is a pulsar in a moderately relativistic orbit with, most likely, a neutron star companion. One PK parameter, the relativistic advance of periastron, has been measured. A timing analysis was published by Thorsett *et al.* (1993), and updated by Arzoumanian (1995). Using data from early 1985 to late 1994, we find an improved value $\dot{\omega} = 0.01019(13)^\circ\text{yr}^{-1}$, yielding a total system mass $M = 2.64 \pm 0.05M_\odot$ and the constraints $m_1 < 1.44M_\odot$ and $m_2 > 1.20M_\odot$. Using a uniform prior distribution in $\sin i$, we find the central 68% confidence intervals $m_1 = 1.30_{-0.46}^{+0.13}$ and $m_2 = 1.34_{-0.13}^{+0.47}$ and central 95% confidence intervals $m_1 = 1.30_{-1.08}^{+0.18}$ and $m_2 = 1.34_{-0.15}^{+1.08}$.

3.2. Neutron star/white dwarf binaries

3.2.1. PSR J0437–4715

PSR J0437–4715 is the brightest and closest known millisecond pulsar, and therefore one of the best studied. It has a mass function $f = 1.243 \times 10^{-3} M_{\odot}$, and a white dwarf companion that has been detected optically (Johnston *et al.* 1993, Bailyn 1993, Bell, Bailes, and Bessell 1993, Danziger, Baade, and Della Valle 1993); and both thermal and nonthermal X-ray emission from the neutron star have been observed (Becker and Trümper 1993, Halpern, Martin, and Marshall 1996). The distance is known, $d = 178 \pm 26$ pc, from the effects of parallax on the pulsar timing signal (Sandhu *et al.* 1997). Using the optical data of Danziger *et al.*, Hansen and Phinney (1998b) found an effective temperature of the companion $T_{\text{eff}} = 4600 \pm 200$ K. Combining the T_{eff} and distance estimates with their cooling curves, they find consistent companion models for all masses $0.15 < m_2 < 0.375 M_{\odot}$. This range encompasses the mass limits derived from the P_b – m_2 relation (§2.2.3), $0.16 < m_2 < 0.23 M_{\odot}$.

The binary orbit is nearly circular, and despite the very high timing precision achieved, no PK timing parameters have been measured. However, the proximity of the pulsar leads to a high proper motion ($\mu = 141$ mas/yr), changing the projected orbital size (§2.3.3) at a rate $\dot{x}/x = 2.43(12) \times 10^{-14}$ (Sandhu *et al.* 1997). The implied limit on the inclination angle is $i < 43^\circ$, or $\sin i < 0.682$.

Attempts to measure the system geometry using the polarization of the radio beam (§2.3.1) have proven difficult, because of the very complex emission pattern. Well-calibrated intensity and polarization data have been reported by Manchester and Johnston (1995), who have modeled the sweep of the linear polarization position angle across the profile in terms of the rotating vector model. They find that an impact parameter of the line of sight on the magnetic pole $\beta = -5^\circ$ and an angle between the line of sight and the spin axis $\zeta = 140^\circ$ produced reasonable agreement with the data, but there are strong systematic deviations from the simple rotating vector model. Using the same data, Gil and Krawczyk (1997) model the multicomponent profile and find a comparable impact parameter, $\beta = -4^\circ$, but a very different $\zeta = 16^\circ$. They show that this geometry also explains the observed polarization sweep over much of the pulse period. With the assumption that the pulsar spin axis is aligned with the orbital axis, the implied orbital inclination is $\sin i = 0.64$ (Manchester and Johnston model) or $\sin i = 0.28$ (Gil and Krawczyk model). Either is consistent with the timing data.

The timing limit on $\sin i$, together with the mass function and the upper limit on m_2 from the core mass–orbital period relation, gives an upper limit to the pulsar mass of $m_1 < 1.51 M_{\odot}$, while the optical upper limit on m_2 gives only the much weaker limit $m_1 <$

$3.29M_{\odot}$. The Manchester and Johnston inclination together with the P_b - m_2 mass range gives $0.77 < m_1 < 1.37M_{\odot}$, while the Gil and Krawczyk inclination gives $0.11 < m_1 < 0.23M_{\odot}$, a physically implausible result. In any case, the complexity of the pulse shape modeling leads us to adopt the weaker one-sided limit $m_1 < 1.51M_{\odot}$.

Improvements of the parallax measurement and the optical photometry and spectroscopy are needed to further constrain the companion mass. An independent mass determination would test the core mass–orbital period relation as well as improve the limit on m_1 . Measurement of the position angle of the ascending node (perhaps through scintillation studies), combined with the measurement of \dot{x}/x , would give the inclination of the orbit.

3.2.2. PSR J1012+5307

PSR J1012+5307 has a hot, bright white dwarf companion that has been extensively studied. van Kerkwijk, Bergeron, and Kulkarni (1996) have used the models of Bergeron, Wesemael, and Fontaine (1991) to determine the effective temperature $T_{\text{eff}} = 8550 \pm 25$ K and surface gravity $\log g = 6.75 \pm 0.07$ of the companion. The latter value is in disagreement with an unpublished value of Callanan and Koester, $\log g = 6.4 \pm 0.2$, quoted by Hansen and Phinney (1998b). Using the optical observations and their cooling models for low mass helium white dwarfs, Hansen and Phinney find a companion mass $0.165 < m_2 < 0.215M_{\odot}$ for the van Kerkwijk *et al.* gravity measurement and $0.13 < m_2 < 0.18$ for the Callanan and Koester value.

The radial velocity of the companion has been measured, making J1012+5307 a double-line spectroscopic pulsar binary. van Kerkwijk *et al.* have found $m_1/m_2 = 9.5 \pm 0.5$ (van Kerkwijk, private communication; their earlier published value $m_1/m_2 = 13.3 \pm 0.7$ was corrupted by a calibration problem). Depending on the gravity measurement, the resulting (1σ) pulsar mass limit is $1.5 < m_1 < 2.2M_{\odot}$ or $1.2 < m_1 < 1.8M_{\odot}$. Clearly resolution of the discrepant gravity measurements must be a high priority, the radial velocity measurements now contribute negligibly to the total error on m_2 . For now, we adopt Hansen and Phinney’s conservative conclusion that $1.2 < m_1 < 2.2M_{\odot}$, and we regard the error range as roughly a 68% confidence interval.

3.2.3. PSR J1045–4509

PSR J1045–4509 is in a 4.08 day orbit with mass function $1.765 \times 10^{-3}M_{\odot}$. The P_b - m_2 relation gives an upper limit to the companion mass of $0.168M_{\odot}$, leading to a limit on the

pulsar mass of $m_1 < 1.48M_\odot$.

3.2.4. PSR J1713+0747

PSR J1713+0747 is a bright pulsar in a nearly circular, 68 day orbit with a white dwarf companion. At the timing precision reached (about 500 ns for 1.4 GHz observations), Camilo (1995) found that the Shapiro PK parameters r and s were required to adequately model the data, but strong covariances between the range parameter r and other orbital parameters (especially x) prevented him from setting interesting limits on the pulsar or companion mass.

The P_b – m_2 relation predicts $0.26 < m_2 < 0.35M_\odot$. Companion mass estimates are also possible by combining unpublished optical observations of the white dwarf by Lundgren *et al.* with the parallax from pulsar timing (Camilo, Foster, and Wolszczan 1994). The resulting limits are $0.15 < m_2 < 0.31M_\odot$ if the white dwarf has a thick H envelope, and $m_2 < 0.27M_\odot$ if it has a thin H envelope (Hansen and Phinney 1998b).

If the observed mass function $f = 7.896 \times 10^{-3}M_\odot$ is combined with the P_b – m_2 limit on m_2 and the restriction $\sin i < 1$, an upper limit to the pulsar mass is found: $m_1 < 1.94M_\odot$. The optical observations yield a tighter limit, $m_1 < 1.63M_\odot$, as was noted by Hansen and Phinney. More interesting limits can be obtained by combining the Shapiro measurements with the limits on m_2 (recalling that $m_2 = r$). For example, if $m_2 = 0.299M_\odot$, the timing data of Camilo is consistent with only the restricted range $\sin i = 0.963(4)$. By letting m_2 vary over the range allowed by the P_b – m_2 relation, we find the allowed pulsar mass $m_1 = 1.45 \pm 0.31$, where the uncertainties are dominated by the systematic uncertainties in the P_b – m_2 relation. If the companion mass is limited to the intersection of the regions allowed by P_b – m_2 and the optical measurements, $0.26 < m_2 < 0.31M_\odot$, then we find $m_1 = 1.34 \pm 0.20M_\odot$.

3.2.5. PSR B1802–07

PSR B1802–07 is in the globular cluster NGC 6539. Its companion is most likely a white dwarf; the system’s large eccentricity can be understood as the result of gravitational perturbations of the system by close stellar encounters in the dense cluster.

The relativistic advance of periastron $\dot{\omega}$ was measured by Thorsett *et al.* (1993), and an improved measurement was published by Arzoumanian (1995). Using the same analysis techniques, with data extending through October 1997, we find a slightly improved value $\dot{\omega} = 0.0578(16)$, implying a total system mass $M = 1.62(7)M_\odot$. The lower bound on the companion mass from the requirement that $\sin i < 1$ is $(fM^2)^{1/3} = 0.29M_\odot$, and the lower

bound on the inclination from the requirement $m_1 > 0$ is $\sin i > (f/M)^{1/3} = 0.18$ (or $i > 10^\circ$). Using a uniform prior for $\sin i$ in the range $0.18 < \sin i < 1$, we find a 68% confidence bound on the pulsar mass $m_1 = 1.26_{-0.17}^{+0.08}M_\odot$ and a 95% confidence bound $m_1 = 1.26_{-0.67}^{+0.15}M_\odot$.

3.2.6. PSR J1804–2718

PSR J1804–2718 is in an 11.1 day orbit. The P_b – m_2 relation limits its companion mass to $0.185 < m_2 < 0.253M_\odot$; the resulting upper limit on the pulsar mass is $m_1 < 1.73M_\odot$.

3.2.7. PSR B1855+09

PSR B1855+09 is a 5.4 ms pulsar in a 12.3 day circular orbit ($e = 2 \times 10^{-5}$) with a white dwarf companion. Because it is a bright pulsar for which high precision timing measurements can be made and because the orbital inclination is high, measurements have been made of the PK parameters r and s .

We have reanalyzed all of the available data, extending from January 1986 to January 1994. (For the data collected after mid-1989, taken with the Princeton Mark III timing system (Stinebring *et al.* 1992), a new algorithm was used for identifying times and frequencies where the signal strength was enhanced by interstellar scintillation and weighting this data in subsequent analysis.) The details and complete timing solution will be published elsewhere. The Shapiro parameters are $r = Gm_2/c^3 = 0.248(11)M_\odot$ and $s = \sin i = 0.9993(2)$. The resulting limits on the pulsar mass are $m_1 = 1.41(10)M_\odot$ (68% confidence; the 95% confidence region will be about twice as large). The new measurement is in good agreement with previous values: $m_1 = 1.27_{-0.15}^{+0.23}M_\odot$ (Ryba and Taylor 1991) and $m_1 = 1.50_{-0.14}^{+0.26}$ (Kaspi, Taylor, and Ryba 1994).³

The P_b – m_2 relation predicts $0.19 < m_2 < 0.26M_\odot$, in good agreement with the timing measurement. The corresponding upper limit to the pulsar mass is $m_1 < 1.51M_\odot$. As noted above, scintillation measurements have also been used to limits $\sin i \geq 0.94$ (Dewey *et al.* 1988).

³Note that both Ryba and Taylor (1991) and Kaspi *et al.* (1994) incorrectly (over)estimate the error on m_1 by calculating the *joint* 68% confidence bound on $r = T_\odot m_2$ and $s = \sin i$ and then interpreting this as a 68% confidence bound on each of m_2 and $\sin i$.

3.2.8. PSR J2019+2425

PSR J2019+2425 is in a 76.5 day orbit. The P_b - m_2 relation gives a limit on the companion mass $0.264 < m_2 < 0.354M_\odot$; the resulting upper limit on the pulsar mass is $m_1 < 1.68M_\odot$.

3.3. Neutron star/main sequence binaries

3.3.1. PSR J0045–7319

The pulsar J0045–7319 is the only known pulsar in the Small Magellanic Cloud. It is in a binary orbit, with mass function $f = 2.17M_\odot$ (Kaspi *et al.* 1994). The companion has been identified as a B1 V star. The radial velocity of the companion has been measured, giving a mass ratio $q = m_2/m_1 = 6.3 \pm 1.2$ (Bell *et al.* 1995) We have compared the observed optical luminosity $L = 1.2 \times 10^4 L_\odot$ and temperature $T_{\text{eff}} = 2.4(1) \times 10^4$ K to the grids of stellar models calculated by Schaller *et al.* (1992) for the low metallicity ($Z = 0.001$) appropriate for the SMC, and estimate the companion mass to be $10 \pm 1M_\odot$. The pulsar mass is then $m_1 = m_2/q = 1.58 \pm 0.34M_\odot$ (68% confidence), where the uncertainty is dominated by the uncertainty in the amplitude of the companion’s radial velocity curve.

4. Discussion

For a dozen neutron stars, useful mass constraints are available with no assumptions beyond the applicability of the general relativistic equations of orbital motion to binary pulsar systems. Ten of these stars are members of double neutron star binaries. With the possible exception of PSR B2127+11C, in the globular cluster M15, the pulsar in each system is believed to have undergone a short period of mass accretion during a high-mass X-ray binary phase ($\Delta m \sim 10^{-3}M_\odot$, Taam and van den Heuvel 1986). The companion stars have not undergone accretion; their masses most directly preserve information about the initial mass function of neutron stars.

Only two “millisecond” pulsars, the end products of extended mass transfer in low-mass X-ray binaries, have interesting mass estimates based on GR alone: PSRs B1802–07 and B1855+09. Because such pulsars must accrete $\sim 0.1M_\odot$ to reach millisecond periods (Taam and van den Heuvel 1986), and much more ($\sim 0.7M_\odot$) in some field decay models (e.g., van den Heuvel and Bitzaraki 1995), obtaining additional mass measurements of millisecond pulsars is of particular interest in testing evolutionary models and in locating the maximum

neutron star mass.

As noted in §2.2.3, the P_b – m_2 relation can be used to estimate the companion mass in recycled binary systems with circular orbits and orbital periods $P_b \gtrsim 3$ d. There are now thirteen such millisecond ($P_{\text{spin}} < 10$ ms) pulsars known, excluding those in globular clusters (where gravitational interactions may have significantly perturbed the orbital parameters since spin-up). In each case, the measured mass function and the inferred companion mass, together with the requirement that $\sin i < 1$, then yields an upper limit on the mass of the pulsar itself. A number of systems in which this upper limit is particularly constraining have been mentioned in §3.2.

Additional constraints on the neutron star mass in these systems can be derived using statistical arguments, given a prior assumption about the distribution of binary inclinations. The simplest such assumption is that the binaries are randomly oriented on the sky, though biases toward high or low inclinations are possible in some models (§2.3.4). However, as discussed below, we believe there is currently no evidence for such a bias, so for the remainder of this discussion we assume random orbital orientations.

For an individual system, we are interested in the probability distribution⁴ $p(m_1; f, P_b)$ for the neutron star mass m_1 given the measured mass function f and binary period P_b . We can neglect the measurement uncertainty in f and P_b . Then, the probability distribution for m_1 can be written schematically as

$$p(m_1; f, P_b) = \int_0^1 d(\cos i) \int_{m_{2,\min}(P_b)}^{m_{2,\max}(P_b)} dm_2 p(m_2; P_b) p(\cos i) p(m_1 | m_2, \cos i; f), \quad (16)$$

where $m_1 = f^{-1/2}(m_2 \sin i)^{3/2} - m_2$ is restricted to positive values. We have evaluated this numerically for each system, assuming that $p(\cos i)$ is uniform between zero and unity and that $p(m_2; P_b)$ is uniformly distributed within the appropriate factor (see §2.2.3) of the m_2 implied by equations (9)–(11). Not surprisingly, the width of the distribution $p(m_1; f, P_b)$ is dominated by the range of allowed $\cos i$ rather than the uncertainty in m_2 for a given P_b . For each of the 13 binaries, we have plotted the cumulative distribution $\text{CDF}(m_1) = \int_0^{m_1} p(m'_1) dm'_1$ in Figure 1.

The median and 68% and 95% confidence regions for each pulsar mass is given in Table 2. Although several of the pulsars have, under the assumptions made, most likely masses well above $2M_\odot$, some such results are expected even if all the masses are quite low. In fact, in

⁴We adopt the notation that $p(x; A)$ is the (marginal) probability density for the random variable x , where x depends upon the parameter A . Also, $p(x|y; A)$ is the conditional probability density for the random variable x for a given value of the random variable y and parameter A .

only one case of the 13 pulsars does $1.35M_{\odot}$ lie outside the 95% central confidence region (J1045–4509), and in 6 cases of 13 is $1.35M_{\odot}$ excluded at 68% confidence, consistent with chance.

It is interesting to ask whether a single, simple distribution of neutron star masses is consistent with all of our observational constraints. We considered two models for this question: a Gaussian distribution of masses with mean \hat{m} and standard deviation σ , and a uniform distribution of masses between m_l and m_u (*cf.* Finn 1994). A maximum likelihood analysis was used to estimate the parameters \hat{m} , σ , m_l , and m_u (assuming a uniform prior distribution for all four parameters). The resulting 68% and 95% joint confidence limits on \hat{m} and σ are shown in Figure 2, and on m_l and m_h in Figure 3. In each model, the distribution of neutron star masses is remarkably narrow: the maximum likelihood solutions are $\hat{m} = 1.35M_{\odot}$ and $\sigma = 0.04M_{\odot}$, and $m_l = 1.26M_{\odot}$ and $m_u = 1.45M_{\odot}$.

Of course, *any* model (even a poor one) will yield maximum likelihood parameters for a given data set. However, it is obvious by inspection that both the Gaussian and uniform distributions for the neutron star mass are good fits to the extremely narrow observed range of neutron star masses in the double neutron star binaries. While it is difficult to quantify the goodness-of-fit for the entire data set, because of the diverse assumptions made in the various mass estimates and the sometimes highly non-gaussian error estimates, we can easily test some neutron star subsamples against the maximum likelihood gaussian model $m_1 = 1.35 \pm 0.04M_{\odot}$. For the thirteen neutron-star–white-dwarf binaries, we used a Monte Carlo technique to evaluate the fit quality. For each binary (with its measured P_b and f), we simulated a large number of Monte Carlo trials where the neutron star mass m_1 was drawn from the maximum likelihood model, m_2 was drawn from the appropriate uniform distribution implied by P_b , and $\cos i$ was drawn from a uniform distribution. The Monte Carlo trials were then used to construct the probability distribution for the mass function, and this distribution was used to compute the cumulative probability for the measured mass function, $p(f' < f)$. If the model and the associated assumptions are correct, then the cumulative probabilities for the 13 measured mass functions should be consistent with a uniform distribution between zero and unity (*cf.* a classical V/V_{\max} test, Schmidt 1968). A KS test of the distribution shows consistency with a uniform distribution at the improbably good 99% level (Figure 4).

For the ten stars for which gaussian error estimates σ_e are available (both stars in the relativistic binaries B1534+12, B1913+16, and B2127+11C, as well as J1012+5307, J1713+0747, B1855+09, and J0045–7319), we can calculate a χ^2 statistic, $\sum(m - \hat{m})^2 / (\sigma^2 + \sigma_e^2) = 7.5$, consistent with expectations for a chi-square distribution with $10 - 2$ degrees of freedom.

We conclude, therefore, that at least in the radio pulsar systems, there is no evidence for neutron star masses above about $1.45M_{\odot}$. Indeed, the data appear very well modeled by very narrow distributions centered around $1.35M_{\odot}$.

5. Summary

There are now 26 neutron stars in binary radio pulsar systems for which useful mass constraints can be derived. Of these, about half are neutron star-white dwarf binaries in which the mass determination depends on the validity of the P_b - m_2 relation and the isotropy of the binary orbits with respect to the line-of-sight, as discussed in the previous section. All other mass constraints are listed in Table 3 and shown in Figure 5.

Although we defer a full discussion of the underlying neutron star mass distribution and its implications for neutron star formation and evolution until after analysis of the X-ray binary systems (Paper II), we note here a few points of particular interest about the radio pulsar binaries. Figure 5 is striking primarily for the very small variations in the masses of well measured stars. This has, of course, been noted before (e.g., Thorsett *et al.* 1993), but it remains surprising that no new mass measurements differ greatly from $1.4M_{\odot}$. In the five double neutron star binaries for which a relativistic periastron advance yields an accurate total (and hence average) mass, the average neutron star masses vary by less than 7%.

The most surprising implication of the current results is that there is little evidence for mass transfer of $0.1M_{\odot}$ or more in the millisecond pulsar systems. It is important, then, to reiterate the assumptions upon which this conclusion rests: (1) the P_b - m_2 is correct, at least within the (modest) claimed precision, and (2) binary orbits are randomly oriented with respect to the line of sight. There are good prospects for testing both assumptions.

The reliability of the P_b - m_2 relation depends principally upon the core-mass-radius relation for red giants (eqns. 10 and 11). The latter relation can be tested observationally by careful study of nearby red giants. Precise measurements of bolometric flux and angular size (through optical/infrared photometry and interferometry; see, for example, Dyck *et al.* 1996, Perrin *et al.* 1998) together with accurate distance measurements (e.g., using *Hipparcos*) can be used to probe the relationship between luminosity and radius. Since the core-mass-luminosity relation for red giants should be inherently more precise than the core-mass-radius relation (Rappaport *et al.* 1995 and references therein), such observations would provide an effective test of the core-mass-radius (and hence P_b - m_2) relation. Further, we hope that the power of the P_b - m_2 relation as a statistical tool will encourage more detailed theoretical investigations of, in particular, the extension of the relation to orbital periods below about

three days, where X-ray heating and bloating of the companion star become important.

Although any technique that limits $\sin i$ (§2.3; e.g., polarization or scintillation studies) can be used to test the hypothesis that orbits are randomly inclined, the most precise measurements will come from pulsar timing and Shapiro time delay measurements. In Table 2 we list the mean predicted amplitude of the Shapiro delay signal $\Delta t_S = 2m_2 T_\odot \log(1 - \sin i)$ for each of the thirteen pulsars discussed in §4, under the assumption that the neutron stars are all $1.4M_\odot$ and the companion masses are the central value predicted by the $P_b - m_2$ relation. Of these systems, only B1855+09 has a well measured signal (Ryba and Taylor 1991, Kaspi, Taylor, and Ryba 1994); it and the less studied J2019+2425 have the largest predicted signals. (It is also interesting to note that of the pulsars in Table 2, the only two that have been clearly shown to have “classical” interpulse emission separated from the main radio emission peak by $\sim 180^\circ$ are B1855+09 and J1804–2718. These are two of the four pulsars that the $P_b - m_2$ relation suggests are observed on lines of sight that are most nearly equatorial, as would be expected for systems in which both magnetic poles are seen.)

An assumed pulsar mass distribution and the $P_b - m_2$ relation allow us to test our assumption that the orbital inclinations are randomly distributed: i.e., $\cos i$ is uniformly distributed. In Figure 4 we show the cumulative distribution of $\cos i$ for the thirteen pulsar–white-dwarf binaries discussed above, using $\sin i$ values from Table 2 except for B1855+09, for which a better estimate is available from timing. We find that the measured values are consistent with uniform at the 81% level. Because the pulsar spin and orbital angular momenta are most likely aligned, we further conclude that there is no evidence for either alignment or counteralignment of pulsar magnetic fields in millisecond pulsars, contrary to some predictions (e.g., Ruderman 1991).

The observations on which this paper is based were carried out by many people. SET particularly thanks his collaborators Z. Arzoumanian, D. J. Nice, and J. H. Taylor. V. M. Kaspi, L. Rawley, and M. Ryba all contributed significantly to the PSR B1855+09 dataset, as did A. Vasquez and other staff members of the Arecibo Observatory, operated by Cornell University for the U. S. National Science Foundation. Observations were also made with the facilities of the National Radio Astronomy Observatory. We thank M. H. van Kerkwijk for sharing results in advance of publication, and D. C. Backer for valuable discussions. The research of SET is supported by the NSF. DC is supported by a NASA Compton GRO Postdoctoral Fellowship, under grant NAG 5-3109.

REFERENCES

- Arzoumanian, Z. 1995, PhD thesis, Princeton University.
- Baade, W. and Zwicky, F. 1934, *Phys. Rev.*, 45, 138.
- Backer, D. C. 1998, *ApJ*, 493, 873.
- Bailyn, C. D. 1993, *ApJ*, 411, L83.
- Becker, W. and Trümper, J. 1993, *Nature*, 365, 528.
- Bell, J. F., Bailes, M., and Bessell, M. S. 1993, *Nature*, 364, 603.
- Bell, J. F., Bessell, M. S., Stappers, B. W., Bailes, M., and Kaspi, V. M. 1995, *ApJ*, 447, L117.
- Bergeron, P., Wesemael, F., and Fontaine, G. 1991, *ApJ*, 367, 253.
- Camilo, F. 1995, PhD thesis, Princeton University.
- Camilo, F., Foster, R. S., and Wolszczan, A. 1994, *ApJ*, 437, L39.
- Chakrabarty, D. and Thorsett, S. E. 1998, in preparation.
- Cordes, J. M. 1986, *ApJ*, 311, 183.
- Damour, T. and Deruelle, N. 1986, *Ann. Inst. H. Poincaré (Physique Théorique)*, 44, 263.
- Damour, T. and Taylor, J. H. 1992, *Phys. Rev. D*, 45, 1840.
- D’Antona, F. and Mazzitelli, I. 1990, *ARA&A*, 28, 139.
- Danziger, I. J., Baade, D., and Della Valle, M. 1993, *AA*, 276, 382.
- Deich, W. T. S. and Kulkarni, S. R. 1996, in *Compact Stars in Binaries: IAU Symposium 165*, ed. J. van Paradijs, E. P. J. van del Heuvel, and E. Kuulkers, (Dordrecht: Kluwer), 279.
- Dewey, R. J., Cordes, J. M., Wolszczan, A., and Weisberg, J. M. 1988, in *Radio Wave Scattering in the Interstellar Medium, AIP Conference Proceedings No. 174*, ed. J.M. Cordes, B. J. Rickett, and D. C. Backer, (New York: American Institute of Physics), 217.
- Dyck, H. M., Benson, J. A., van Belle, G. T., & Ridgway, S. T. 1996, *AJ*, 111, 1705.

- Eadie, W. T., Drijard, D., James, F. E., Roos, M., and Sadoulet, B. 1971, *Statistical Methods in Experimental Physics*, (Amsterdam: North-Holland).
- Finn, L. S. 1994, *Phys. Rev. Lett.*, 73, 1878.
- Friedman, J. L., Ipser, J. R., Durisen, R. H., and Parker, L. 1988, *Nature*, 336, 560.
- Gil, J. and Krawczyk, A. 1997, *MNRAS*, 285, 561.
- Halpern, J. P., Martin, C., and Marshall, H. L. 1996, *ApJ*, 462, 908.
- Hansen, B. M. S. and Phinney, E. S. 1998a, *MNRAS*, 294, 557.
- Hansen, B. M. S. and Phinney, E. S. 1998b, *MNRAS*, 294, 569.
- Hulse, R. A. and Taylor, J. H. 1975, *ApJ*, 195, L51.
- Jenet, F. A., Cook, W. R., Prince, T. A., and Unwin, S. C. 1997, *PASP*, 109, 707.
- Johnston, S. *et al.* 1993, *Nature*, 361, 613.
- Johnston, S., Manchester, R. N., Lyne, A. G., Bailes, M., Kaspi, V. M., Qiao, G., and D’Amico, N. 1992, *ApJ*, 387, L37.
- Johnston, S., Walker, M. A., and Bailes, M. 1996. *Pulsars: Problems and Progress, IAU Colloquium 160*, San Francisco. Astronomical Society of the Pacific.
- Jones, A. W. and Lyne, A. G. 1988, *MNRAS*, 232, 473.
- Joss, P. C., Rappaport, S., and Lewis, W. 1987, *ApJ*, 319, 180.
- Kaspi, V. M., Johnston, S., Bell, J. F., Manchester, R. N., Bailes, M., Bessell, M., Lyne, A. G., and D’Amico, N. 1994, *ApJ*, 423, L43.
- Kaspi, V. M., Taylor, J. H., and Ryba, M. 1994, *ApJ*, 428, 713.
- Lorimer, D. R., Lyne, A. G., Bailes, M., Manchester, R. N., D’Amico, N., Stappers, B. W., Johnston, S., and Camilo, F. 1996, *MNRAS*, 283, 1383.
- Lundgren, S. C., Camilo, F., and Foster, R. S. 1996, In Johnston *et al.* 1996, p. 497.
- Lyne, A. G. 1984, *Nature*, 310, 300.
- Manchester, R. N. and Johnston, S. 1995, *ApJ*, 441, L65.
- Manchester, R. N. and Taylor, J. H. 1977, *Pulsars*, (San Francisco: Freeman).

- Navarro, J., Manchester, R. N., Sandhu, J. S., Kulkarni, S. R., and Bailes, M. 1997, ApJ, 486, 1019.
- Nice, D. J., Sayer, R. W., and Taylor, J. H. 1996, ApJ, 466, L87.
- Oppenheimer, J. R. and Volkoff, G. 1939, Phys. Rev., 55, 374.
- Perrin, G., Coudé du Foresto, V., Ridgway, S. T., Mariotti, J.-M., Traub, W. A., Carleton, N. P., & Lacasse, M. G. 1998, A&A, 331, 619.
- Podsiadlowski, P. 1991, Nature, 350, 136.
- Rappaport, S. and Joss, P. C. 1997, ApJ, 486, 435.
- Rappaport, S., Podsiadlowski, P., Joss, P. C., DiStefano, R., and Han, Z. 1995, MNRAS, 273, 731.
- Refsdal, S. and Weigert, A. 1971, AA, 13, 367.
- Reid, I. N. 1996, AJ, 111, 2000.
- Rickett, B. J. 1988, in *Radio Wave Scattering in the Interstellar Medium*, AIP Conference Proceedings No. 174, ed. J.M. Cordes, B. J. Rickett, and D. C. Backer, (New York: American Institute of Physics), 2.
- Ruderman, M. 1991, ApJ, 366, 261.
- Ryba, M. F. 1991, PhD thesis, Princeton University.
- Ryba, M. F. and Taylor, J. H. 1991, ApJ, 371, 739.
- Sandhu, J. S., Bailes, M., Manchester, R. N., Navarro, J., Kulkarni, S. R., and Anderson, S. B. 1997, ApJ, 478, L95.
- Sayer, R. W. 1996, PhD thesis, Princeton University.
- Schaller, G., Schaerer, D., Meynet, G., and Maeder, A. 1992, A&AS, 96, 269.
- Schmidt, M. 1968, ApJ, 151, 393.
- Shrauner, J. A., Stairs, I. H., Dewey, R. J., Krumholz, M., Taylor, H. E., Taylor, J. H., and Thorsett, S. E. 1996, in Johnston *et al.* 1996, p. 23.
- Stairs, I. H., Arzoumanian, Z., Camilo, F., Lyne, A. G., Nice, D. J., Taylor, J. H., Thorsett, S. E., and Wolszczan, A. 1998, ApJ, submitted; astro-ph/9712296.

- Stinebring, D. R., Kaspi, V. M., Nice, D. J., Ryba, M. F., Taylor, J. H., Thorsett, S. E., and Hankins, T. H. 1992, *Rev. Sci. Inst.*, 63, 3551.
- Taam, R. E. and van den Heuvel, E. P. J. 1986, *ApJ*, 305, 235.
- Taylor, J. H. 1987, in *General Relativity and Gravitation*, ed. M. A. H. MacCallum, (Cambridge: Cambridge University Press), 209.
- Taylor, J. H. 1992, *Phil. Trans. Roy. Soc. London A*, 341, 117.
- Taylor, J. H., Manchester, R. N., Lyne, A. G., and Camilo, F. 1995, Unpublished (available at <ftp://pulsar.princeton.edu/pub/catalog>).
- Taylor, J. H. and Weisberg, J. M. 1989, *ApJ*, 345, 434.
- Thorsett, S. E., Arzoumanian, Z., McKinnon, M. M., and Taylor, J. H. 1993, *ApJ*, 405, L29.
- Thorsett, S. E., Arzoumanian, Z., and Taylor, J. H. 1993, *ApJ*, 412, L33.
- Thorsett, S. E. and Stinebring, D. R. 1990, *ApJ*, 361, 644.
- van den Heuvel, E. P. J. 1994, *A&A*, 291, L39.
- van den Heuvel, E. P. J., and Bitzaraki, O. 1995, *A&A*, 297, L41.
- van Kerkwijk, M. H. 1996, in Johnston *et al.* 1996, p. 489.
- van Kerkwijk, M. H., Bergeron, P., and Kulkarni, S. R. 1996, *ApJ*, 467, L89.
- Webbink, R. F., Rappaport, S., and Savonije, G. J. 1983, *ApJ*, 270, 678.
- Wheeler, J. A. 1966, *ARA&A*, 4, 393.

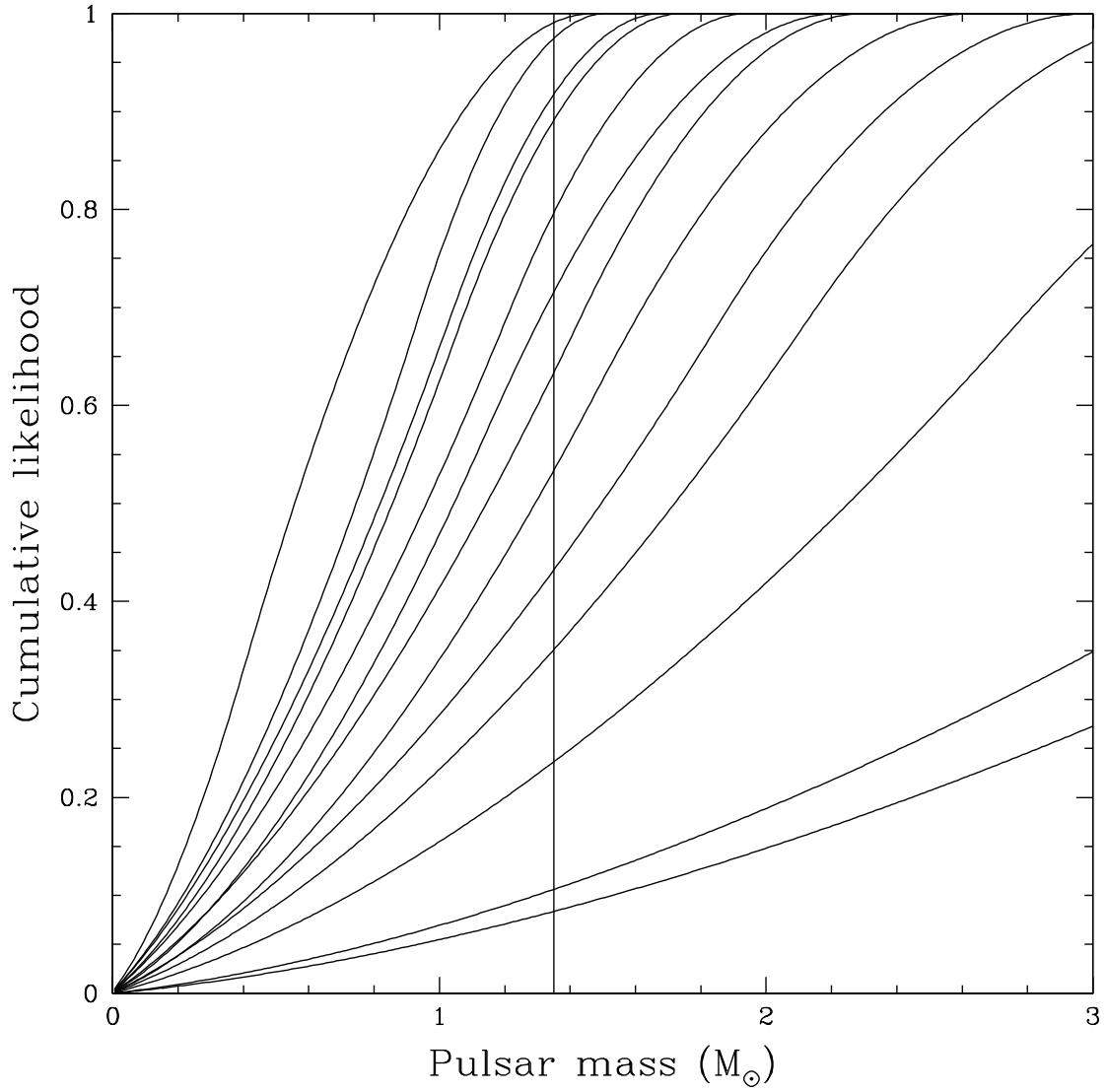


Fig. 1.— Cumulative probabilities $\int dm_1 p(m_1; f, P_b)$ for the 13 pulsars in Table 2, as described in the text. A vertical line is shown at $1.35M_{\odot}$.

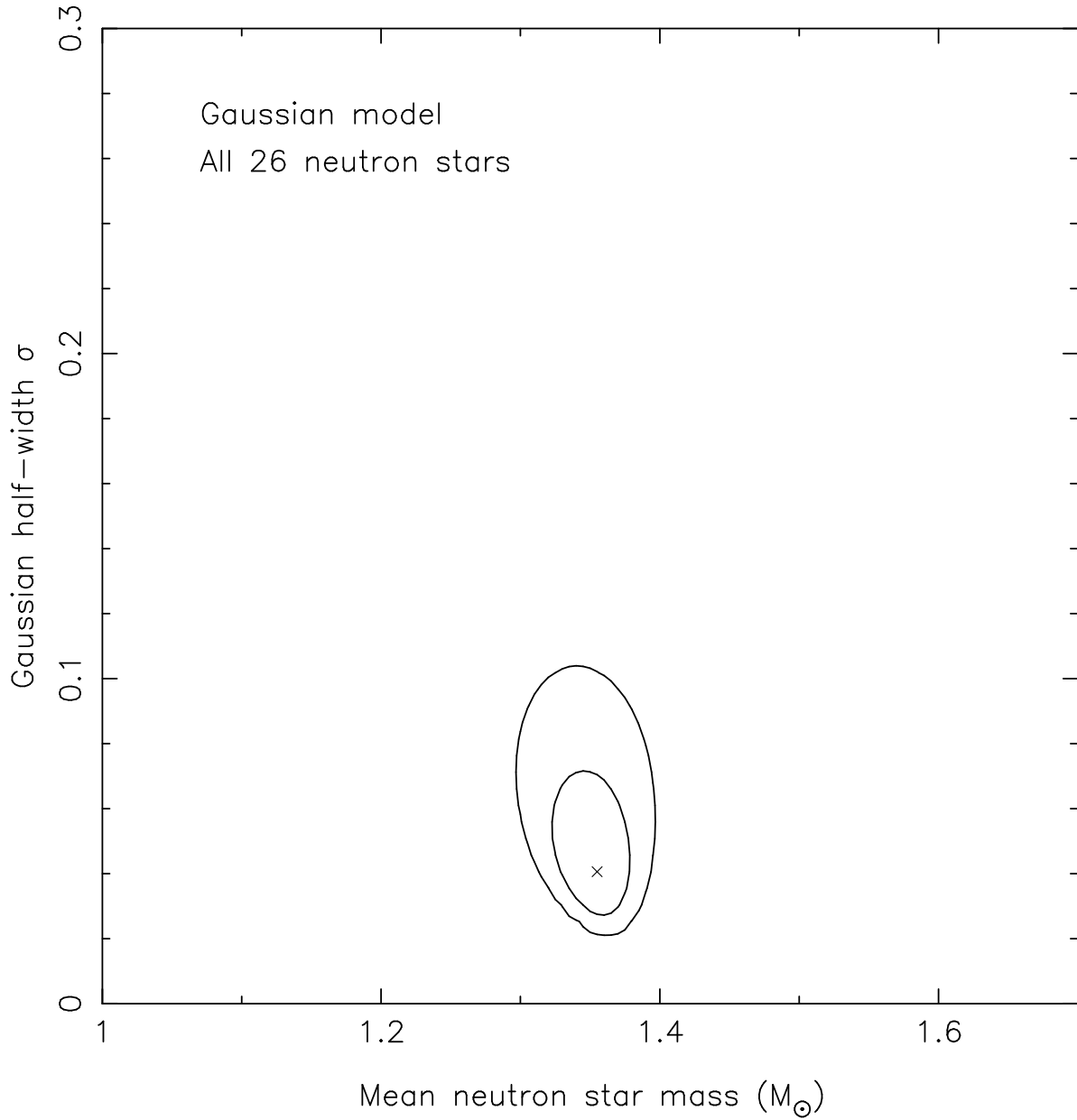


Fig. 2.— Maximum likelihood estimate of the mean and standard deviation, \hat{m} and σ , of a gaussian neutron star mass distribution. The maximum likelihood solution is marked with a cross, and contours indicate 68% and 95% confidence regions.

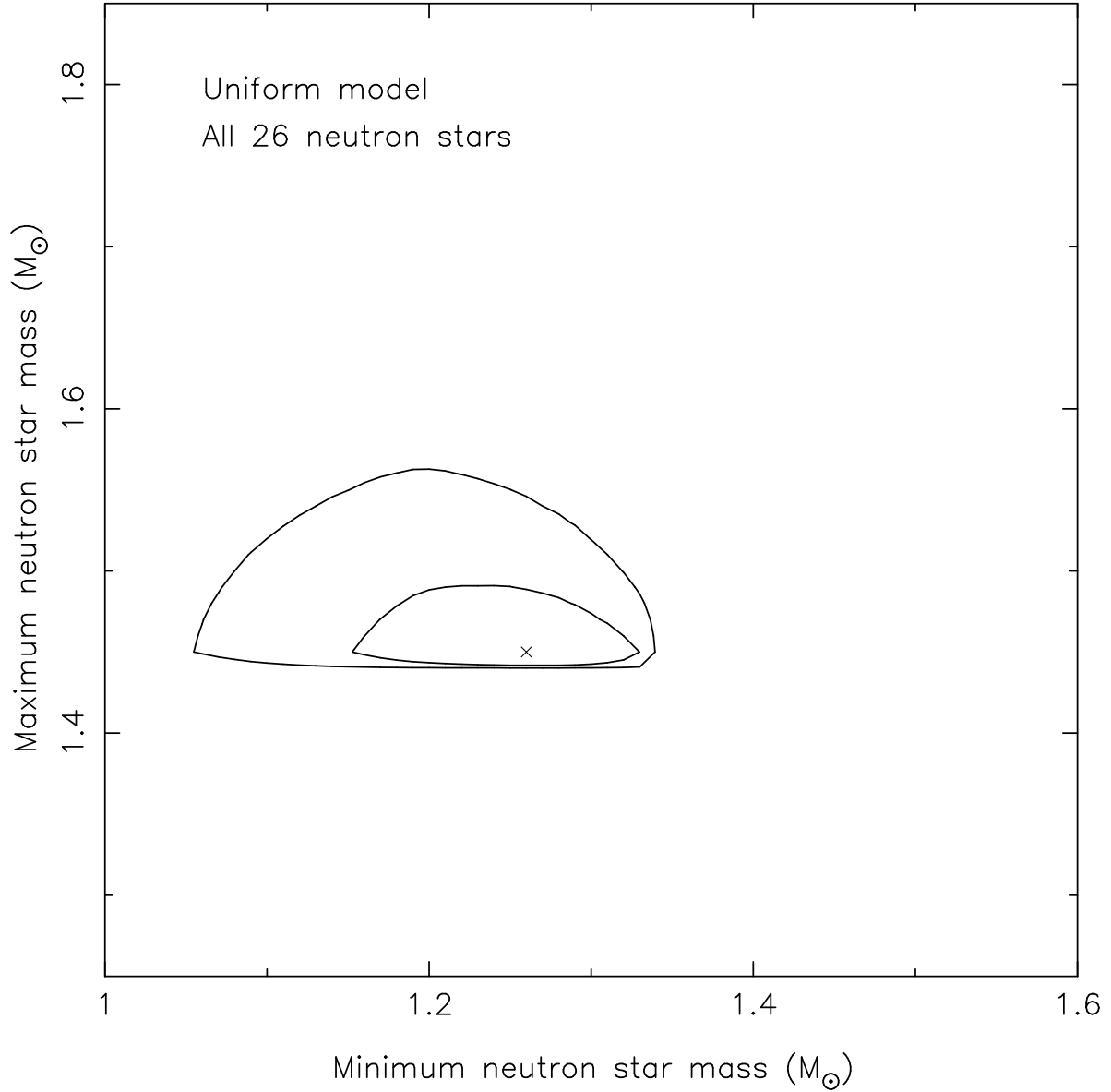


Fig. 3.— Maximum likelihood estimate of the minimum and maximum neutron star mass, m_l and m_u , assuming masses are uniformly distributed between the upper and lower bounds. The maximum likelihood solution is marked with a cross, and contours indicate 68% and 95% confidence regions.

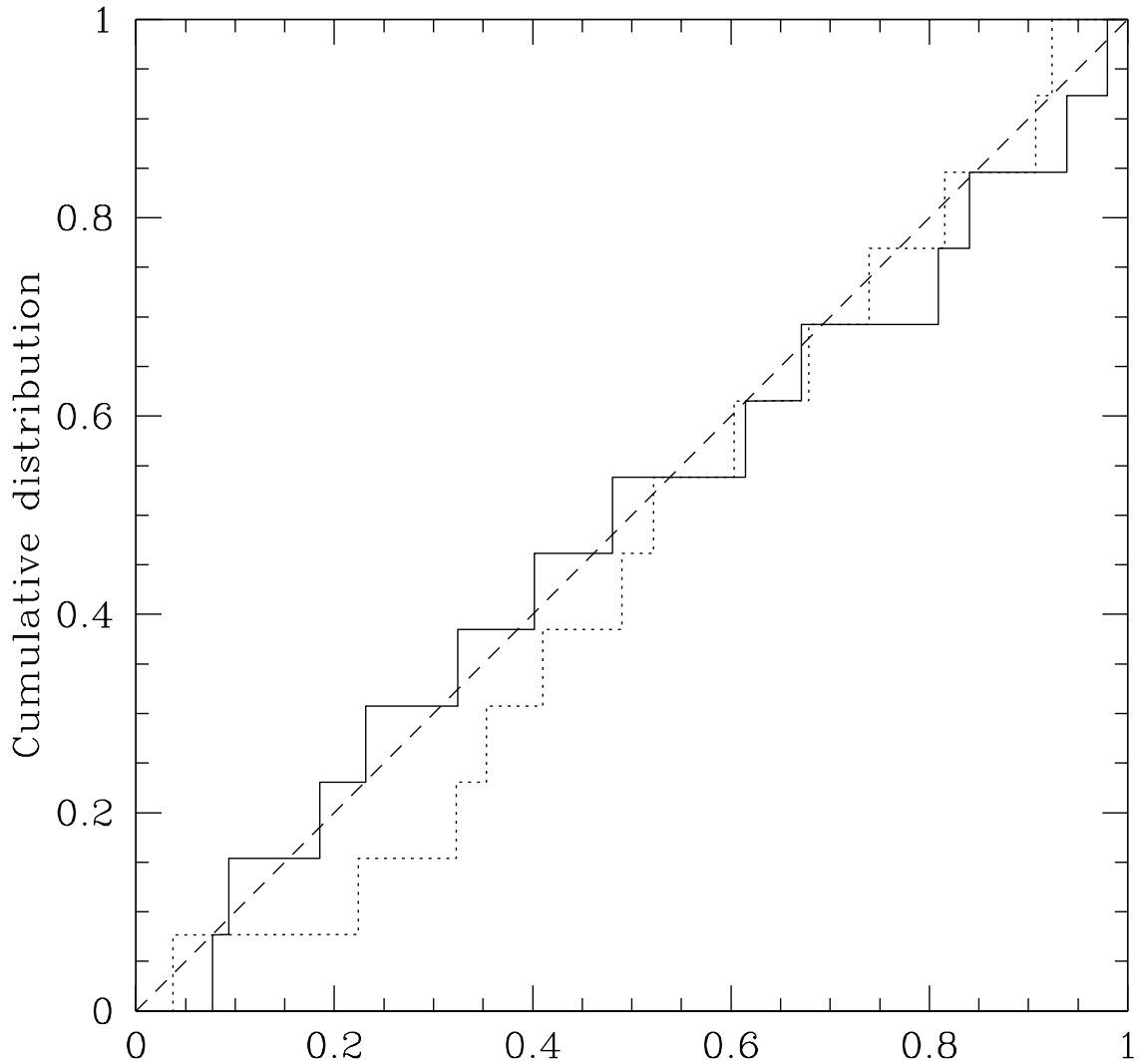


Fig. 4.— Cumulative distribution of $p(f' < f)$ (solid line, §4) and of $\cos i$ (dotted line, §5) for the thirteen millisecond pulsars with $P_b > 3$ days and $P < 10$ ms, assuming a pulsar mass distribution $m_1 = 1.35 \pm 0.04M_\odot$ and companion mass distribution as predicted by the P_b – m_2 relation (see text). Each distribution is consistent with uniform (dashed line, KS probability of 99% and 81%, respectively), as expected if orbital inclinations are randomly distributed and the P_b – m_2 relation correctly predicts the companion mass distribution.

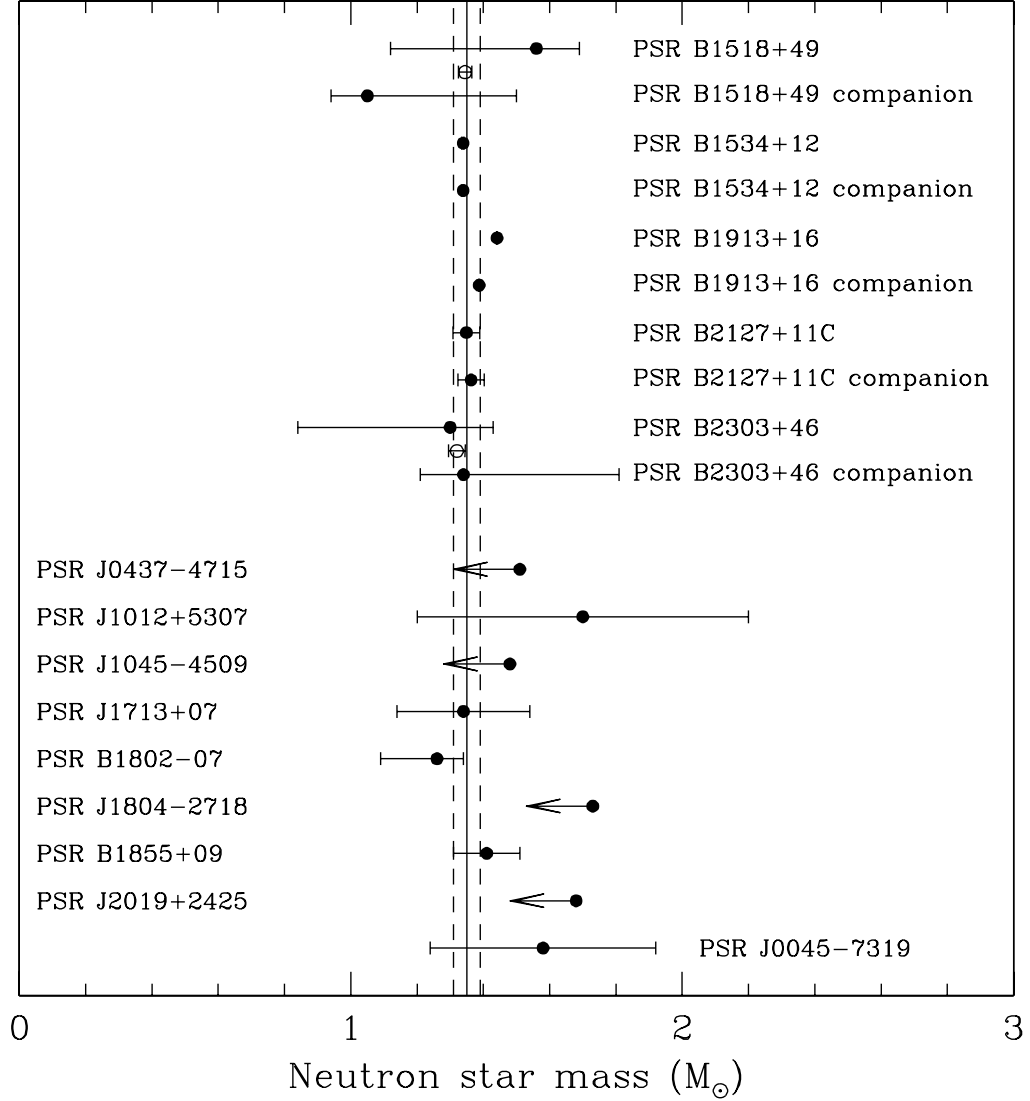


Fig. 5.— Neutron star masses from observations of radio pulsar systems. All error bars indicate central 68% confidence limits, except upper limits are one-sided 95% confidence limits. Five double neutron star systems are shown at the top of the diagram. In two cases, the average neutron star mass in a system is known with much better accuracy than the individual masses; these average masses are indicated with open circles. Eight neutron-star–white-dwarf binaries are shown in the center of the diagram, and one neutron-star–main-sequence-star binary is shown at bottom. Vertical lines are drawn at $m = 1.35 \pm 0.04M_{\odot}$.

Table 1. Binary radio pulsar systems^a

PSR name	P_{spin} (s)	P_b (d)	e	Notes
<i>Double neutron star binaries</i>				
J1518+4904	0.040935	8.634	0.24948	
B1534+12	0.037904	0.421	0.27368	
B1913+16	0.05903	0.323	0.61713	
B2127+11C	0.030529	0.335	0.68141	1
B2303+46	1.066371	12.34	0.65837	
<i>Neutron star/white dwarf binaries</i>				
B0021–72E	0.003536	2.257	0.000	1
B0021–72I	0.003485	0.226	0.00	1
B0021–72J	0.002101	0.121	0.00	1
J0034–0534	0.001877	1.589	0.0000	
J0218+4232	0.002323	2.029	0.00000	
J0437–4715	0.005757	5.741	0.00000	
J0613–0200	0.003062	1.199	0.00000	
B0655+64	0.195671	1.029	0.00000	
J0751+1807	0.003479	0.263	0.0000	
B0820+02	0.864873	1232.47	0.01187	
J1012+5307	0.005256	0.605	0.00000	
J1022+10	0.016453	7.805	0.0001	
J1045–4509	0.007474	4.084	0.00000	
B1310+18	0.033163	255.8	0.002	1
J1455–3330	0.007987	76.175	0.00017	
J1603–7202	0.014842	6.309	0.0000	2
B1620–26	0.011076	191.443	0.02531	1,4
J1640+2224	0.003163	175.461	0.0008	
B1639+36B	0.003528	1.259	0.005	1
J1643–1224	0.004622	147.017	0.00051	
J1713+0747	0.004570	67.825	0.00007	
B1718–19	1.004037	0.258	0.000	1
B1744–24A	0.011563	0.076	0.0000	1
B1800–27	0.334415	406.781	0.00051	
B1802–07	0.023101	2.617	0.212	1

Table 1—Continued

PSR name	P_{spin} (s)	P_b (d)	e	Notes
J1804–2717	0.009343	11.129	0.00004	2
B1820–11	0.279828	357.762	0.79462	3
B1831–00	0.520954	1.811	0.000	
B1855+09	0.005362	12.327	0.00002	
J1910+0004	0.003619	0.141	0.00	1
J1911–1114	0.003626	2.717	0.0000	2
B1953+29	0.006133	117.349	0.00033	
B1957+20	0.001607	0.382	0.00000	
J2019+2425	0.003935	76.512	0.00011	
J2033+17	0.005949	56.2	0.00	
J2129–5721	0.003726	6.625	0.0000	2
J2145–0750	0.016052	6.839	0.00002	
J2229+2643	0.002978	93.016	0.00026	
J2317+1439	0.003445	2.459	0.00000	
<i>Neutron star/main sequence binaries</i>				
J0045–7319	0.926276	51.169	0.808	
B1259–63	0.047762	1236.724	0.86993	
<i>Pulsar with planetary mass companions</i>				
B1257+12	0.006219	66.536	0.0182	
	2nd planet	98.223	0.0264	

^aUnless otherwise indicated, all data are from the 1995 revision of the Princeton Pulsar Catalog (Taylor *et al.* 1995).

Note. — (1) Believed to be a globular cluster member; (2) Lorimer *et al.* 1996; (3) may be a double neutron star system; (4) probably a triple system (Thorsett, Arzoumanian, and Taylor 1993).

Table 2. Mass estimates from the P_b - m_2 relation.

Pulsar	P_b (days)	f ($10^{-3}M_\odot$)	m_2^a (M_\odot)	Pulsar mass ^b (M_\odot)					Predicted: ^c	
				95% lower	68% lower	median	68% upper	95% upper	$\sin i$	Δt_S (μs)
J0437–4715	5.741	1.243	0.164	0.106	0.472	1.044	1.573	1.971	0.87	3.5
J1045–4509	4.083	1.765	0.132	0.047	0.234	0.557	0.965	1.273	0.97	6.2
J1455–3330	76.174	6.272	0.305	0.098	0.491	1.144	1.681	2.058	0.85	5.9
J1640+2224	175.460	5.907	0.351	0.135	0.651	1.495	2.190	2.681	0.73	4.6
J1643–1224	147.017	0.783	0.341	0.553	2.106	4.439	6.335	7.674	0.38	1.6
J1713+0747	67.825	7.896	0.299	0.078	0.405	0.960	1.419	1.741	0.91	7.6
J1804–2718	11.128	4.137	0.212	0.073	0.369	0.856	1.265	1.558	0.94	6.7
B1855+09	12.327	5.557	0.219	0.060	0.315	0.745	1.101	1.351	0.97	9.0
B1953+29	117.349	2.417	0.328	0.236	1.024	2.251	3.251	3.955	0.58	2.8
J2019+2425	76.511	10.686	0.305	0.062	0.338	0.818	1.218	1.500	0.95	10.0
J2033+17	56.2	2.75	0.290	0.172	0.772	1.720	2.489	3.029	0.67	3.2
J2129–5721	6.625	1.049	0.176	0.138	0.591	1.293	1.900	2.348	0.80	2.7
J2229+2643	93.015	0.839	0.315	0.463	1.789	3.787	5.409	6.552	0.42	1.7

^aCentral value from P_b - m_2 relation, eqn. 9 and eqns. 10 and 11.

^bMedian and central 68% and 95% confidence bounds.

^cMean value of $\sin i$ and Shapiro delay amplitude $\Delta t_S = 2m_2T_\odot \log(1 - \sin i)$, assuming a gaussian underlying neutron star mass distribution $m_1 = 1.35 \pm 0.04$ and uniform m_2 in the range allowed by the P_b - m_2 relation (§5).

Table 3. Radio pulsar mass summary

Star	Median mass (M_{\odot})	68% central imits	95% central limits	Notes ^a
<i>Double neutron star binaries</i>				
J1518+4904				
pulsar	1.56	+0.13/ – 0.44	+0.20/ – 1.20	GR, RO
companion	1.05	+0.45/ – 0.11	+1.21/ – 0.14	GR, RO
average	1.31	± 0.035	± 0.07	GR
B1534+12				
pulsar	1.339	± 0.003	± 0.006	GR
companion	1.339	± 0.003	± 0.006	GR
B1913+16				
pulsar	1.4411	± 0.00035	± 0.0007	GR
companion	1.3874	± 0.00035	± 0.0007	GR
B2127+11C				
pulsar	1.349	± 0.040	± 0.080	GR
companion	1.363	± 0.040	± 0.080	GR
average	1.3561	± 0.0003	± 0.0006	GR
B2303+46				
pulsar	1.30	+0.13/ – 0.46	+0.18/ – 1.08	GR, RO
companion	1.34	+0.47/ – 0.13	+1.08/ – 0.15	GR, RO
average	1.32	± 0.025	± 0.05	GR
<i>Neutron star/white dwarf binaries</i>				
J0437–4715	< 1.51	\dot{x} , $P_b m_2$
J1012+5307	1.7	± 0.5	± 1.0	Opt
J1045–4509	< 1.48	$P_b m_2$
J1713+0747	1.45	± 0.31	± 0.62	$P_b m_2$, GR
	1.34	± 0.20	± 0.40	$P_b m_2$, GR, Opt
B1802–07	...	< 1.39	< 1.45	GR
	1.26	+0.08/ – 0.17	+0.15/ – 0.67	GR, $P_b m_2$
J1804–2718	< 1.73	$P_b m_2$
B1855+09	1.41	± 0.10	± 0.20	GR
J2019+2425	< 1.68	$P_b m_2$
<i>Neutron star/main sequence binaries</i>				
J0045–7319	1.58	± 0.34	± 0.68	Opt, MS

^aAssumptions made in mass estimate: (GR) general relativistic binary model; (RO) random orbital orientation, or inclination angle uniform in $\cos i$; ($P_b m_2$) core mass orbital period relation; (\dot{x}) proper-motion-induced change in the projected semi-major axis; (Opt) optical companion observations; (MS) main sequence stellar model.